Supplementary Information

Black Phosphorus Quantum Dots as Dual-Functional Electron Selective Materials for Efficient Plastic Perovskite Solar Cells

Nianqing Fu,[a]* *Chun Huang,*[b] *Peng Lin,*[b] *Mingshan Zhu,*[c] *Tao Li,*[b] *Mao Ye,*[b] *Shenghuang Lin,*[d]* *Guoge Zhang,*[a] *Jun Du,*[a] *Chang Liu,*[e] *Baomin Xu,*[e] *Danyang Wang,*[f] *and Shanming Ke,*[b,g]*

[a] School of Materials Science and Engineering, South China University of Technology, Guangzhou 510640, China.

[b]Guangdong Research Center for Interfacial Engineering of Functional Materials, College of Materials Science and Engineering, Shenzhen University, Shenzhen, 518060, China.

[c] School of Environment, Jinan University, Guangzhou 510632, P. R. China.

[d] Department of Applied Physics, The Hong Kong Polytechnic University, Hong Kong, China.

[e] Department of Materials Science and Engineering, South University of Science and Technology, Shenzhen 518055, China.

[f] School of Materials Science and Engineering, The University of New South Wales, Sydney, New South Wales 2052, Australia.

[g] School of Materials Science and Engineering, Nanchang University, Nanchang 330031, Jiangxi, China.

Corresponding authors:

Dr. N. Q. Fu, E-mail: msnqfu@scut.edu.cn

Dr. S. Ke, E-mail: smke@szu.edu.cn

Dr. S. Lin, E-mail: shenghuanglinchina@gmail.com

Table S1. A survey of rigid and flexible PSCs employing low-temperature processed electron selective layer (ESL).

ESL materials	Processing route	Processing temperature	Substrate	Device configuration[a]	Efficiency	Published year	Ref. No.
PCBM	Solution-processed	Room T	Flexible	Inverted	**9.4**	2014	S1
					18.1%	2017	S2
Organic molecular CDIN	Solution-processed	100 °C	Flexible	Normal	**14.2%**	2016	S3
Solid-State Ionic-Liquids	Solution-processed	70 °C	Flexible	Normal	**16.09%**	2016	S4
Al_2O_3	Solution-processed	150 °C	Rigid	Normal	**12.3%**	2013	S5
TiO_2	ALD+UV-irradiation	Room T	Flexible	Normal	**7.4%**	2015	S6
	Solution-process photonic curing	80 °C	Flexible	Normal	**11.2%**	2016	S7
	Magnetron sputtering	Room T	Flexible	Normal	**15.07%**	2015	S8
	Magnetron sputtering	Room T	Flexible	Normal	**15.8%**	2017	S9
	Electron beam evaporated	100 °C	Flexible	Normal	**13.5%**	2015	S10
Nb-doped TiO_2	UV-assisted solution process	＜50 °C	Flexible	Normal	**16.01%**	2016	S11
Hydrogen doping TiO_2+PCBM	magnetron sputtering	Room T	Rigid	Normal	**19.3%**	2017	S12
ZnO	Solution-processed	150 °C	Flexible	Normal	**11%**	2015	S13
	Solution-processed	150 °C	Flexible	Normal	**15.6%**	2016	S14

	Solution-processed particles	150 °C	Rigid	Mesoporous	**18.9%**	2017	S15
SnO_2	ALD	100 °C	Flexible	Normal	**15%**	2016	S16
	ALD+water vapor treatment	100 °C	Flexible	Normal	**17.08%**	2017	S17
	Solution-processed	150 °C	Rigid	Normal	**19.9%**	2016	S18
Sb-doped SnO_2	Solution-processed	100 °C	Rigid	Normal	**17.7%**	2016	S19
Li-doped SnO_2	Solution-processed	185 °C	Flexible	Normal	**14.78%**	2016	S20
Zn_2SnO_4	Solution-processed	100 °C	Flexible	Normal	**14.85%**	2015	S21
	Solution processed + particle	100 °C	Flexible	Mesoporous	**16%**	2016	S22
WO_x	Solution-processed	Room T	Rigid	Normal	**14.9%**	2015	S23
In_2O_3	Solution-processed	200 °C	Rigid	Normal	**14.39%**	2017	S24
Nb_2O_5	E-beam evaporated	Room T	Flexible	Normal	**15.56%**	2017	S25
In_2S_3	Chemical bath	100 °C	Rigid	Normal	**18.22%**	2017	S26
BPQDs	Solution-processed	60 °C	Rigid	Normal	**14.6%**	This work	
			Flexible	Normal	**11.26%**	This work	

[a] "Normal" represents that the PSCs were built in a planar structure

Reference

S1 J. You, Z. Hong, Y. (Michael) Yang, Q. Chen, M. Cai, T.-B. Song, C.-C. Chen, S.g Lu, Y. Liu, H. Zhou and Y. Yang, *ACS Nano*, 2014, **8**, 1674-1680.

S2 C. Bi, B. Chen, H. Wei, S. DeLuca and J. Huang, *Adv. Mater.* 2017, **29**, 1605900.

S3 Z. Zhu, J.-Q. Xu, C.-C. Chueh, H. Liu, Z. Li, X. Li, H. Chen and A. K.-Y. Jen, *Adv. Mater.*, 2016, **28**, 10786-10793.

S4 D. Yang, R. Yang, X. Ren, X. Zhu, Z. Yang, C. Li and S. (Frank) Liu, *Adv. Mater.*,

2016, **28**, 5206-5213.

S5 J. M. Ball, M. M. Lee, A. Hey and H. J. Snaith, *Energy Environ. Sci.*, 2013, **6**, 1739-1743.

S6 F. Di Giacomo, V. Zardetto, A. D'Epifanio, S. Pescetelli, F. Matteocci, St. Razza, A. D. Carlo, S. Licoccia, W. M. M. Kessels, M. Creatore and T. M. Brown, *Adv. Energy Mater.*, 2015, **5**, 1401808.

S7 S. Das, G. Gu, P. C. Joshi, B. Yang, T. Aytug, C. M. Rouleau, D. B. Geoheganc and K. Xiao, *J. Mater. Chem. A*, 2016, 4, 9685-9690.

S8 D. Yang, R. Yang, J. Zhang, Z. Yang, S. (Frank) Liu and C. Li, *Energy Environ. Sci.*, 2015, **8**, 3208-3214.

S9 S. S. Mali, C. K. Hong, A. I. Inamdar, H. Imb and S. E. Shim, *Nanoscale*, 2017, **9**, 3095-3104.

S10 W. Qiu, U. W. Paetzold, R. Gehlhaar, V. Smirnov, H.-G. Boyen, J. G. Tait, B. Conings, W. Zhang, C. B. Nielsen, I. McCulloch, L. Froyen, P. Heremans and D. Cheynsa, *J. Mater. Chem. A*, 2015, **3**, 22824-22829.

S11 I. Jeong, H. Jung, M. Parkb, J. S. Park, H. J. Son, J. Joo, J. Lee, M. J. Ko, *Nano Energy*, 2016, **28**, 380-389.

S12 X. Yao, J. Liang, Y. Li, J. Luo, B. Shi, C. Wei, D. Zhang, B. Li, Y. Ding, Y. Zhao and X. Zhang, *Adv. Sci.*, 2017, **4**, 1700008.

S13 J. Zhang, E. José Juárez-Pérez, I. Mora-Seró, B. Viana and T. Pauporté, *J. Mater. Chem. A*, 2015, **3**, 4909-915.

S14 J. H. Heo, M. H. Lee, H. J. Han, B. R. Patil, J. S. Yub and S. H. Im, *J. Mater. Chem. A*, 2016, **4**, 1572-1578.

S15 J. Song, L. Liu, X.-F. Wang, G. Chen, W. Tian and T. Miyasakac, *J. Mater. Chem. A*, 2017, **5**, 13439-13447.

S16 C. Wang, D. Zhao, C. R. Grice, W. Liao, Y. Yu, A. Cimaroli, N. Shrestha, P. J. Roland, J. Chen, Z. Yu, P. Liu, N. Cheng, R. J. Ellingson, X. Zhao and Y. Yan, *J. Mater. Chem. A*, 2016, **4**, 12080-12087.

S17 C. Wang, L. Guan, D. Zhao, Y. Yu, C. R. Grice, Z. Song, R. A. Awni, J. Chen, J. Wang, X. Zhao, and Y. Yan, *ACS Energy Lett.*, 2017, **2**, 2118-2124.

S18 Q. Jiang, L. Zhang, H.Wang, X. Yang, J. Meng, H. Liu, Z. Yin, J.Wu, X. Zhang and J. You, *Nat. Energy*, 2016, **14**, 16177.

S19 Y. Bai, Y. Fang, Y. Deng, Q. Wang, J. Zhao, X. Zheng, Y. Zhang and J. Huang, *ChemSusChem*, 2016, **9**, 2686-2691.

S20 M. Park, J.-Y. Kim, H. J. Son, C.-H. Lee, S. Soon Jang, M. J. Ko, *Nano Energy*, 2016, **26**, 208-215.

S21 S. S. Shin, W. S. Yang, J. H. Noh, J. H. Suk, N. J. Jeon, J. H. Park, J. S. Kim, W. M. Seong and S. Il Seok, *Nat. Commmun.*, 2015, **6**, 7410.

S22 S. S. Shin, W. S. Yang, E. J. Yeom, S. J. Lee, N. J. Jeon, Y.-C. Joo, I. J. Park, J. H. Noh, and S. Il Seok, *J. Phys. Chem. Lett.*, 2016, **7**, 1845-1851.

S23 Y. Hou, C. O. R. Quiroz, S. Scheiner, W. Chen, T. Stubhan, A. Hirsch, M. Halik, and C. J. Brabec, *Adv. Energy Mater.*, 2015, **5**, 1501056.

S24 P. Chen, X. Yin, M. Que, X. Liu and W. Que, J. Mater. Chem. A, 2017, **5**, 9641-9648.

S25 J. Feng, Z. Yanga, D. Yang, X. Ren, X. Zhu, Z. Jin, W. Zi, Q. Wei, S. (Frank) Liu, *Nano Energy*, 2017, **36**, 1-8.

S26 Y. Hou, X. Chen, S. Yang, Y. L. Zhong, C. Li, H. Zhao, H. G. Yang, *Nano Energy*, 2017, **36**, 102-109.

The generation of Tauc Plot and extraction of Eg value:

The bandgap of a semiconductor can be expressed as $\alpha h\nu = C(h\nu - E_g)^n$ or $\left(\frac{Ah\nu}{K}\right)^{1/n} = h\nu - E_g$

Where α is the absorption coefficient (m^{-1}), v is frequency of the light (s^{-1}), h is the Plank's constant (6.626×10^{-34} J s), E_g is the bandgap energy (eV), A is the absorbance of the UV-Vis spectrum, C and K are proportionality constants, n is an exponent which has values of 1/2, 3/2, 2, and 3 for direct allowed, direct forbidden, indirect allowed, and indirect forbidden transitions.

Therefore, the correlation, $(\alpha h\nu)^{1/n}$ vs. $h\nu$-E_g, can be able to get the bandgap energy (E_g) by plotting $(\alpha h\nu)^{1/n}$ and $h\nu$-E_g as y and x axis, respectively. The proportionality constants C and K determine only the y value rather than the linear fit region. Since the BP is a direct bandgap semiconductor, the n value is 2 here. Once the linear fit is obtained, the E_g of the BPQDs can be then determined from the intercept of the linear fit in the lower energy absorption region of the plot of $(\alpha h\nu)^{1/n}$ vs. $h\nu$-E_g.

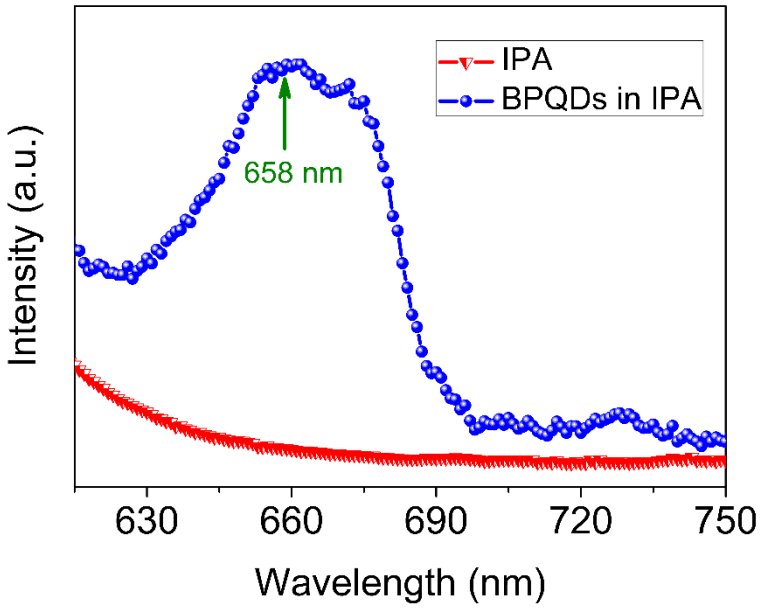

Fig. S1 Steady-state photoluminescence (PL) spectrometry of isoproponal (IPA) and BPQDs in IPA. Excitation wavelength of the laser source is 550 nm.

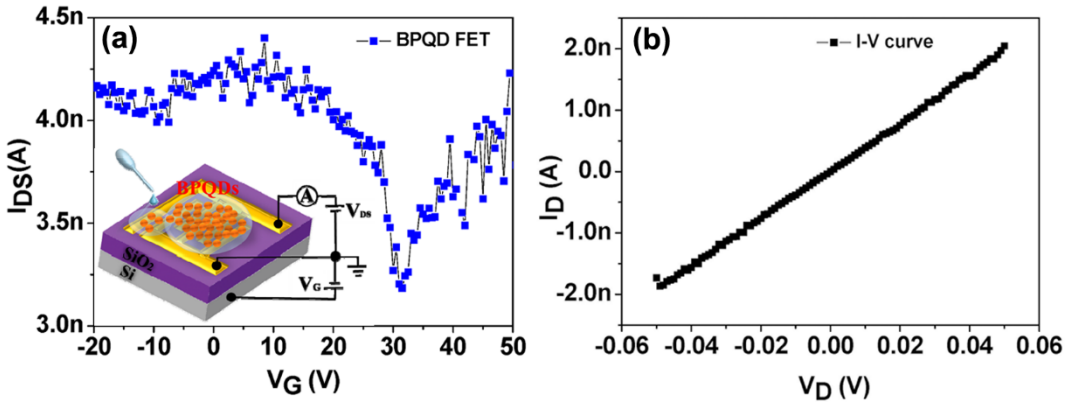

Fig. S2. **(a)** A typical room-temperature I-V curve of the BPQDs based FET. The inset reveals the device structure of BPQDs FET. **(b)** ID-VD curve of the FET.

Experimental details:

The transfer characteristics of the FET are measured at room temperature using the configuration presented as insert in Fig. S1a. For this measurement, metal contacts (gold) were first deposited on SiO_2/Si substrate by standard photolithography process to form bare gold contacts devices through a stencil mask aligned with the substrate. After that, a drop of BPQD solution was drop-casted on the bare devices with only gold interdigitated. The channel length and width of the device is 5 μm and 20 μm respectively. The source-drain V_{DS} was set at 0.1 V while the backgate voltage V_G was varied from -20 V to 50 V.

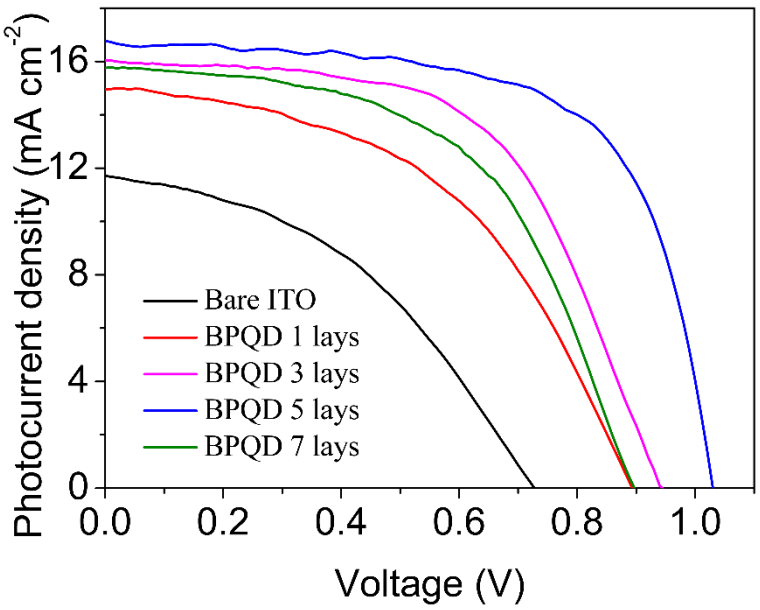

Fig. S3. *J-V* characteristic curves of PSCs built on BPQDs electron selective layer (ESL) with various BPQDs thickness (i.e. 0, 1, 3, 5, 7 layers).

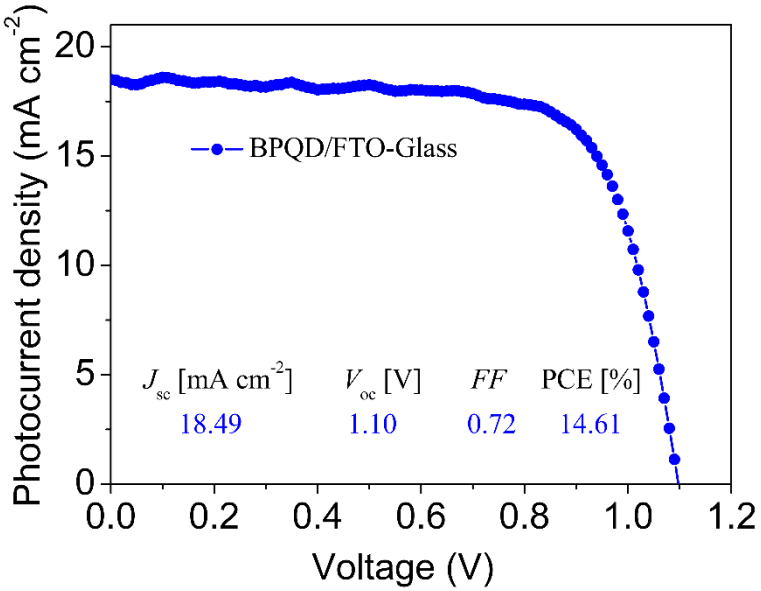

Fig. S4. The *J-V* characteristic curves of rigid FTO/glass substrate based PSCs with a low-temperature produced BPQDs electron selective layer.

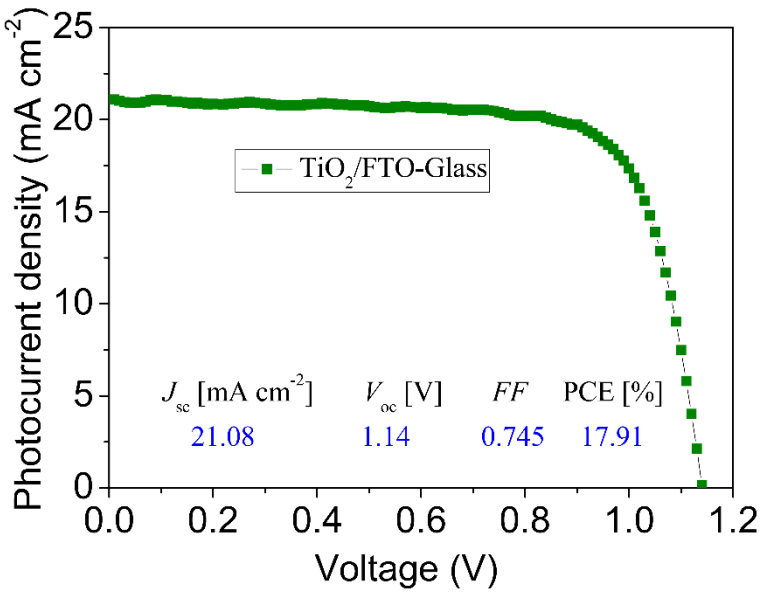

Fig. S5. The *J-V* characteristic curves of rigid FTO/glass substrate based PSCs with a high-temperature produced (450 °C) compact TiO_2 electron selective layer.

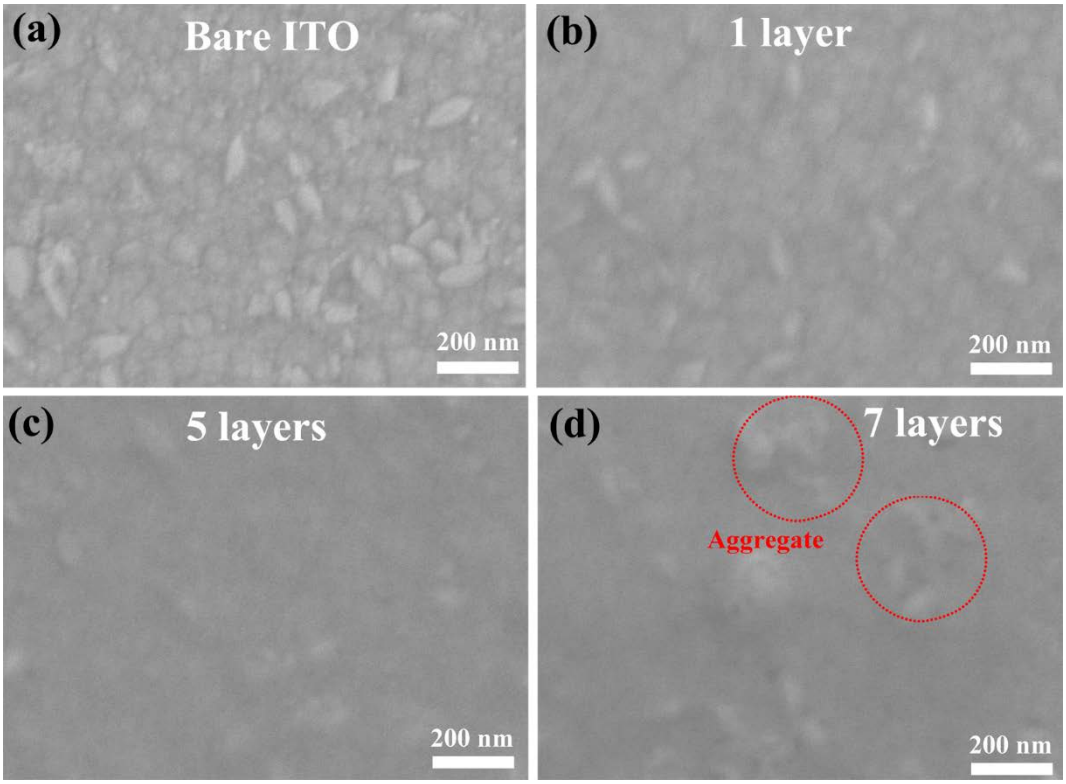

Fig. S6. SEM images of the electrodes with various layers (i.e. 0, 1, 5, 7) of BPQDs deposited on ITO surface.

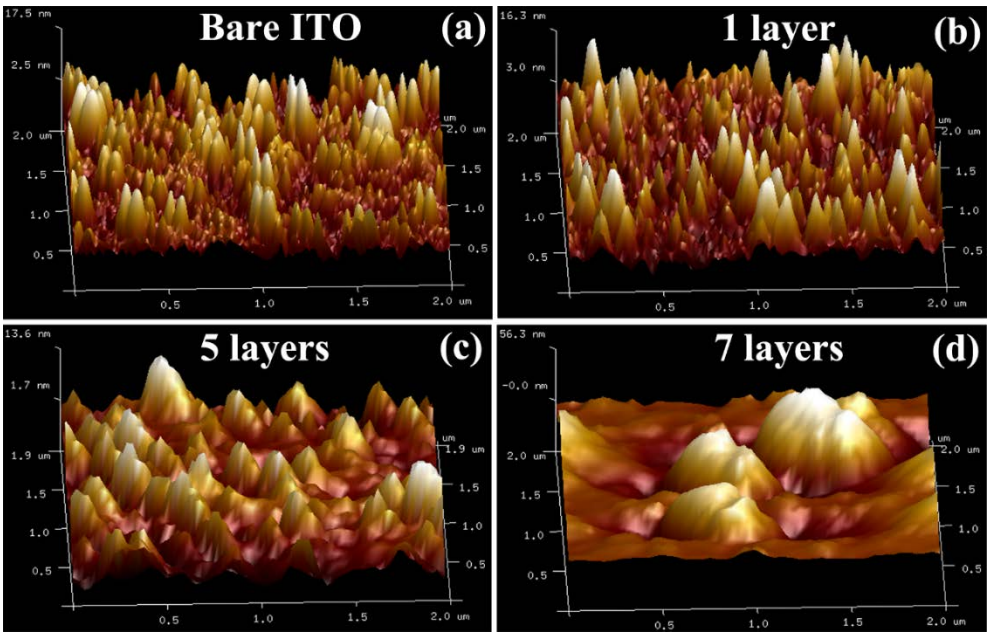

Fig. S7. 3D AFM images of the electrodes with various layers (i.e. 0, 1, 5, 7) of BPQDs deposited on ITO surface.

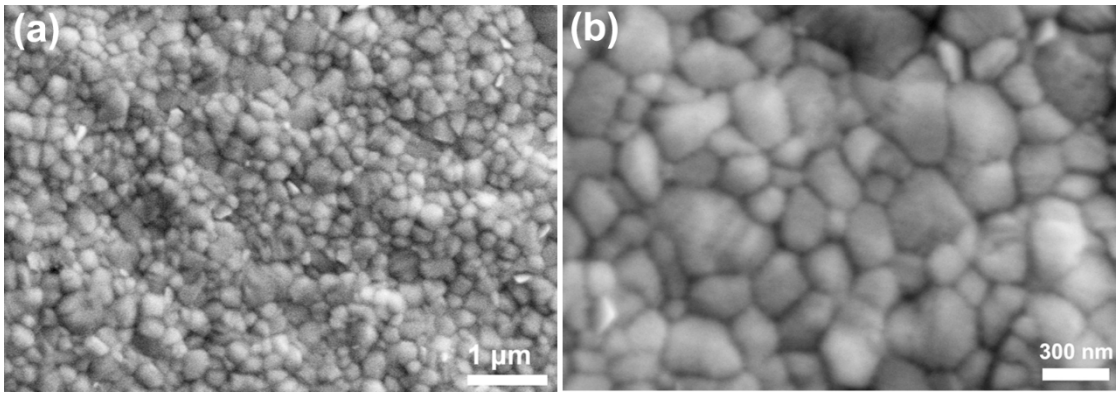

Fig. S8 SEM images of mixed perovskite deposited on low-temperature produced TiO_2 electron selective layer (ESL). The TiO_2 ESL is prepared according to the reported work, Science 2014, 345, 542−546

Table S2. Time resolved photoluminescence characterization of the perovskite electrode built on bare ITO/PEN substrate and BPQDs coated ITO/PEN substrate.[a]

Electrodes	Component 1			Component 2			τ_{ave} (ns)
	τ_1 (ns)	A_1	c_1	τ_2 (ns)	A_2	c_2	
Bare ITO/Perovskite	6.8	958	71.1%	198.2	389	28.9%	184.6
BPQDs/Perovskite	4.3	1334	80.3%	27.6	327	19.7%	18.3

[a]The data were obtained by fitting the TRPL spectra with a bi-exponential decay function of the following form:

$$R(t) = R_0 + A_1 \exp(-\frac{t}{\tau_1}) + A_2 \exp(-\frac{t}{\tau_2})$$

The average lifetime (τ_{ave}) and weight concentration (c) are calculated according to Equation 1 and Equation 2, respectively.

$$\tau_{ave} = \sum_{i=1}^{n} \frac{A_i \tau_i^2}{A_i \tau_i} = \frac{A_1 \tau_1^2 + A_2 \tau_2^2}{A_1 \tau_1 + A_2 \tau_2} \quad \text{(Equation 1)}$$

$$c_i = \frac{A_i}{\sum_{i=1}^{n} A_i} \quad \text{(Equation 2)}$$

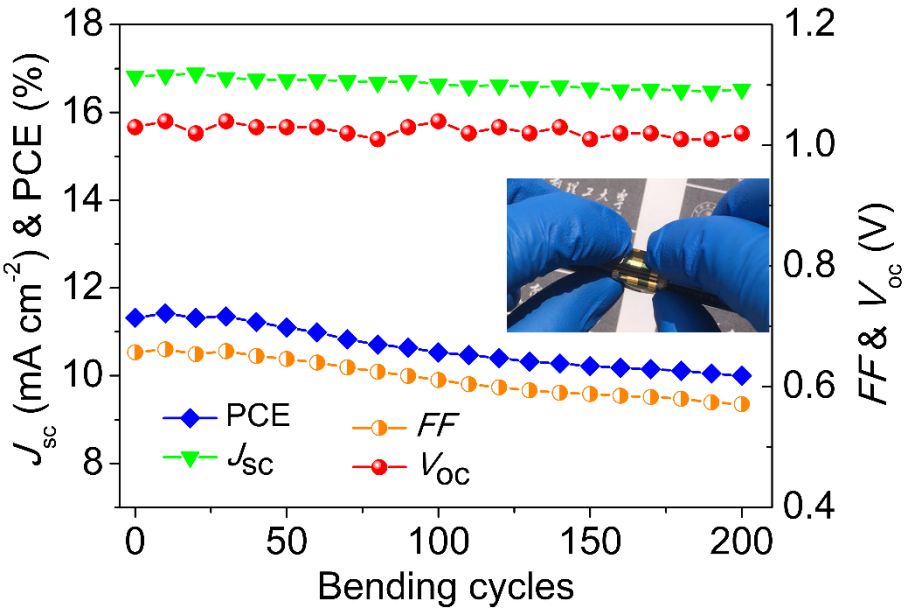

Fig. S9 The photovoltaic parameters variations of the BPQDs-based plastic PSCs as a function of bending cycles.

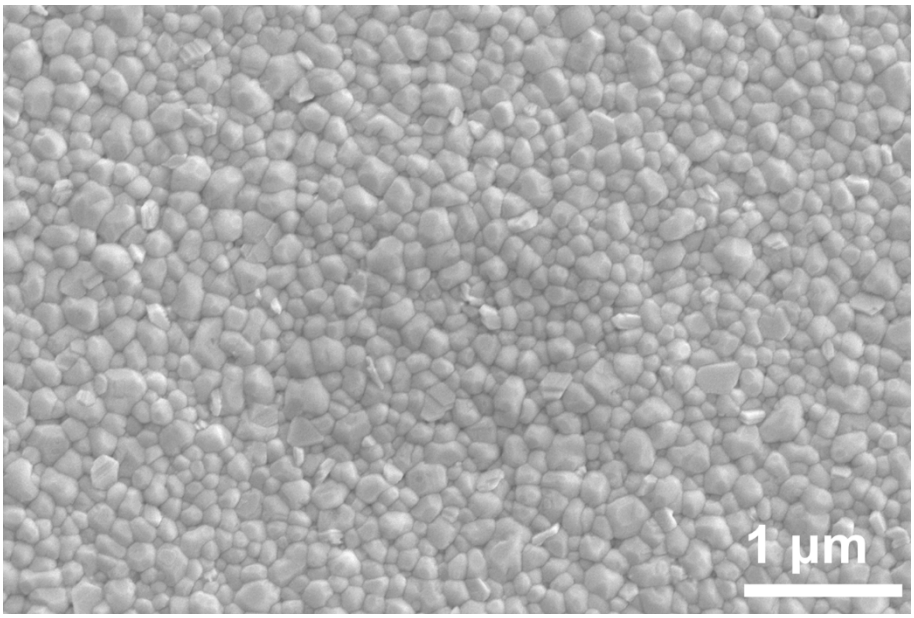

Fig. S10 The SEM images of the perovskite film deposited on BPQDs ESL, after 200 cycles of bending